

Independent phasing of rephasing and non-rephasing 2D electronic spectra

V. P. Singh, A. F. Fidler, B. S. Rolczynski, and G. S. Engel

Citation: *The Journal of Chemical Physics* **139**, 084201 (2013); doi: 10.1063/1.4818808

View online: <http://dx.doi.org/10.1063/1.4818808>

View Table of Contents: <http://scitation.aip.org/content/aip/journal/jcp/139/8?ver=pdfcov>

Published by the AIP Publishing

Articles you may be interested in

[Vibrational dynamics of a non-degenerate ultrafast rotor: The \(C₁₂,C₁₃\)-oxalate ion](#)
J. Chem. Phys. **139**, 164514 (2013); 10.1063/1.4826137

[Terahertz-wave generation in quasi-phase-matched GaAs](#)
Appl. Phys. Lett. **89**, 141119 (2006); 10.1063/1.2357551

[Two-dimensional optical three-pulse photon echo spectroscopy. II. Signatures of coherent electronic motion and exciton population transfer in dimer two-dimensional spectra](#)
J. Chem. Phys. **124**, 234505 (2006); 10.1063/1.2200705

[Two-dimensional electronic spectra of symmetric dimers: Intermolecular coupling and conformational states](#)
J. Chem. Phys. **124**, 124511 (2006); 10.1063/1.2180783

[Electronic coupling and coherences in disordered polymers: Femtosecond 2D-photon echo correlation spectroscopy, signatures of an excitonic two-segmental site system: A theoretical study](#)
J. Chem. Phys. **116**, 8218 (2002); 10.1063/1.1465398



Re-register for Table of Content Alerts

Create a profile.



Sign up today!



Independent phasing of rephasing and non-rephasing 2D electronic spectra

V. P. Singh, A. F. Fidler, B. S. Rolczynski, and G. S. Engel^{a)}

The James Franck Institute, Institute for Biophysical Dynamics, and Department of Chemistry,
The University of Chicago, Chicago, Illinois 60637, USA

(Received 14 June 2013; accepted 5 August 2013; published online 22 August 2013)

Assigning absolute phase to two-dimensional (2D) third-order nonlinear optical signals generally requires acquiring both the rephasing and the non-rephasing signals and comparing the sum of the two to spectrally resolved pump-probe spectra. To date, however, Gradient Assisted Photon Echo Spectroscopy (GRAPES) has only been able to acquire rephasing spectra. Such a constraint requires a new phasing protocol. Here, we analytically prove that the rephasing and non-rephasing spectra can be phased independently using pump-probe signal. We verify this result holds even for finite duration pulses by simulation. This relationship holds for all 2D spectroscopies, not only GRAPES. In addition, we present improvements to GRAPES that enable acquisition of rephasing and non-rephasing signals in different phase-matched directions. We employ our phasing protocol to phase the data for laser dye IR-144, leading to reconstruction of purely absorptive 2D spectrum.

© 2013 AIP Publishing LLC. [http://dx.doi.org/10.1063/1.4818808]

I. INTRODUCTION

Two-dimensional (2D) spectroscopy, a coherent third-order nonlinear spectroscopy, probes coherence and population dynamics on the pico- and femtosecond timescales. Two-dimensional electronic spectroscopy (2DES) has provided new and important information in a variety of systems, including correlations between electrons and holes in bi-exciton states of gallium-arsenide quantum wells,¹ the effects of nanoparticle shape on electronic structure and ultrafast dynamics,² excitation transfer in carbon nanotubes,³ and coherent dynamics in photosynthetic light-harvesting complexes.^{4–6} Detailed reviews of the theory, experimental implementation, and data interpretation of two-dimensional spectroscopies have been published previously.^{7–12} Briefly, interactions between the sample and three excitation pulses result in an oscillating dipolar response, which generates signals in phase-matched directions. By systematically varying the timing between excitation pulses, we can acquire the entire third-order, nonlinear signal.⁸

The recent development of Gradient Assisted Photon Echo Spectroscopy (GRAPES)^{13,14} extends the utility of 2DES by considerably shortening acquisition times, but it poses some unique experimental challenges. For clarity, we refer to conventional experimental approaches for acquiring 2D electronic spectra as “2DES,” and distinguish these from GRAPES.

Both GRAPES and 2DES involve a series of three excitation pulses (pulses 1–3), following a fourth local oscillator (LO) pulse in time using a boxcars geometry. In 2DES, the pulses are focused to a point and the time delay between pulses 1 and 2 (coherence time, τ) and 2 and 3 (population or waiting time, T) are both scanned using linear delay stages. GRAPES obtains the same information, however it only scans

one linear delay stage corresponding to the waiting time. The coherence time delay is resolved by focusing the beams to a line and spatially encoding the timing between pulses 1 and 2 across the sample.^{13,14} Pulse 1 is tilted such that the time delay between pulses 1 and 2 varies. Beams 2 and 3 are parallel, yielding a constant waiting time T at all spatial positions within the sample. This configuration acquires all relevant coherence times simultaneously for each waiting time. The emitted signal is frequency-resolved and imaged onto a charge-coupled device (CCD). The horizontal direction across the CCD detector surface encodes the signal-LO timing in an interferogram along the wavelength dimension, while the vertical dimension on the CCD detector encodes the coherence times.

For perfectly time-ordered system-field interactions, interactions with pulses 1 and 3 generate oscillating dipoles with phase propagating either in common or with opposite sign, resulting in non-rephasing or rephasing signals, respectively. These non-rephasing and rephasing signals are emitted in different phase-matched directions known as the non-rephasing and rephasing directions, respectively. These directions are determined by vector addition of the wavevectors for pulses 1–3. However, the geometry of 2DES experiments permits the acquisition of both of these signals in the same direction by swapping the order of first two pulses. In contrast, GRAPES cannot use this method because the angle between pulses 1 and 3 results in sampling different waiting times along the length of the beam, when beam 2 precedes beam 1 (see Figure S1 of the supplementary material¹⁵). As designed, GRAPES acquires signal in the rephasing phase-matched direction.

Canonical “phasing” procedure, or determining the absolute phase of the 2D spectra, requires acquiring both the rephasing and non-rephasing spectra and comparing their sum to pump-probe spectra. Based on the projection-slice theorem, we prove in Sec. II that rephasing and non-rephasing

^{a)}Author to whom correspondence should be addressed. Electronic mail: gsengel@uchicago.edu

signals can be phased independently by comparing each to the spectrally resolved pump-probe spectra. This proof operates both inside and outside the impulsive limit. We additionally corroborate our phasing procedure with simulation. To further demonstrate the understanding developed in Sec. II, we present in Sec. III a modified GRAPES geometry that acquires signals in both the rephasing and the non-rephasing phase matched directions. The rephasing and the non-rephasing signals acquired in different phase matched directions cannot be simply added and phased in the usual way. However, the signals can be phased independently as demonstrated for laser dye IR 144, and these phased spectra can be scaled and combined to yield the purely absorptive 2D spectrum.

II. THEORY

A frequency-dependent relative phase shift can arise from uncertainties in laser pulse timings and from dispersive components of the experimental apparatus. Because pump-probe signal is unaffected by such effects, it can be used to “phase,”^{8,10} or correct for, the frequency-dependent phase shift the 2D spectra have acquired. Conventionally, the rephasing and non-rephasing signals are summed, and this sum is phased to acquire corrected rephasing and non-rephasing spectra. The objective of this section is to deduce the ability for signals measured in the rephasing and non-rephasing directions to be phased independently from one another using pump-probe data, rather than in sum. This advance is crucial for GRAPES, in which rephasing and non-rephasing spectra cannot be added together in a straightforward manner, due to the different experimental geometries required to acquire each signal.

The theory and experimental implementation of optical nonlinear spectroscopy have been discussed previously in great detail.^{7–12} In this work, we use the definition of the third-order, nonlinear polarization, $P^{(3)}(\vec{\mu}_s, \tau, T, t)$, in the time domain defined by Jonas¹⁶ because it includes explicit integration over arbitrary pulse envelopes rather than interaction times in the impulsive limit. Here, coherence time (τ) and waiting time (T) are defined to be the time delays between the first and second, and between the second and third pulses, respectively. These definitions, which depend only on the time delays between the centers of the pulses, are important to ensure generality of our proof for pulses of finite duration. The center of the third pulse is set as the origin of time t , and $\vec{\mu}_s$ is the direction of signal propagation. The 2D spectrum, $S^{(3)}(\omega_\tau, T, \omega_t)$, is obtained by Fourier transforming the spectrally resolved signal field over coherence time. Thus, ω_τ and ω_t are conjugate variables of τ and t , respectively, related through the Fourier transform.

The spectrally resolved pump-probe spectra, $PP(T, \omega_t)$, and the properly phased 2D spectra, $S^{(3)}(\omega_\tau, T, \omega_t)$, are related by the projection-slice theorem given by¹⁶

$$PP(T, \omega_t) \propto \text{Re} \left\{ \omega_t E_{pr}(\omega_t) \int_{-\infty}^{+\infty} d\omega_\tau S^{(3)}(\omega_\tau, T, \omega_t) \right\}, \quad (1)$$

where $E_{pr}(\omega_t)$ is the electric field of the probe pulse. Following the projection-slice theorem,¹⁷ we rewrite $S^{(3)}(\omega_\tau, T, \omega_t)$ in Eq. (1) as the Fourier transform of $S^{(3)}(\tau, T, \omega_t)$, then rearrange to yield

$$PP(T, \omega_t) \propto \text{Re}\{\omega_t E_{pr}(\omega_t) S^{(3)}(\tau = 0, T, \omega_t)\}. \quad (2)$$

To extend this result to the rephasing spectrum we consider the time-apodized, third-order, nonlinear signal, $\theta(\tau)S^{(3)}(\tau, T, \omega_t)$, where $\theta(\tau)$ is a Heaviside function. After applying the projection-slice theorem to the 2D spectrum of the rephasing signal, we arrive at

$$\theta(0)\text{Re}\{\omega_t E_{pr}(\omega_t) S^{(3)}(\tau = 0, T, \omega_t)\}. \quad (3)$$

Because $\theta(0) = 1$, expression (3) reduces to the $PP(T, \omega_t)$ signal, from Eq. (2). The projection of the signal in the rephasing direction, therefore, equals the spectrally resolved pump-probe signal and can be individually phased. A similar argument can be made for signal in the non-rephasing direction $\tau \leq 0$ simply by apodizing with $\theta(-\tau)$.

This proof holds in both the impulsive and non-impulsive regimes. For perfectly time-ordered interactions in the impulsive limit, the signal in the rephasing direction has contributions only from rephasing Liouville pathways, except for $\tau = 0$ when the rephasing signal has equal contributions from rephasing and non-rephasing Liouville pathways. Application of the projection-slice theorem to the two-dimensional rephasing signal yields the rephasing slice for $\tau = 0$, which is the same as the pump-probe signal.

In the non-impulsive regime, the signal in the rephasing direction has contributions from non-rephasing Liouville pathways when pulses overlap (see Figure S2 of the supplementary material¹⁵). The pump-probe signal acquired using the same pulse bandwidth similarly has contributions from rephasing and non-rephasing Liouville pathways. Thus, it is not intuitive in the non-impulsive limit that the projection of the rephasing signal on the $\omega_\tau = 0$ axis will equal the pump-probe signal. We therefore employ a simulation using pulses of finite duration to demonstrate that signals in the rephasing and non-rephasing directions can indeed be phased independently.

Theoretical calculations of third-order, nonlinear signal, as outlined by Brixner *et al.*,¹⁰ were performed to simulate IR-144 with 30 fs transform-limited pulses centered at 802 nm. System parameters for diffusive dynamics were taken from Joo *et al.*¹⁸ For inertial dynamics, a time constant and coupling strength of 200 fs and 200 cm⁻¹, respectively, were chosen. The signal for zero coherence time was used as the pump-probe signal. In Figure 1, we compare the projections of *a priori* phased signals in the rephasing and non-rephasing directions and find that they are equal to pump-probe signal and to each other, as implied by the proof above. The top row of Figure 1 shows, in order, rephasing, non-rephasing, and comparison of projections of the rephasing and the non-rephasing spectra to pump-probe signal for $T = 0$ fs. The bottom row shows the corresponding spectra for $T = 100$ fs. The projections of rephasing and non-rephasing spectra are shown in red “+” and green circles, respectively, and are found to be equal to pump-probe spectrum (brown squares) as expected.

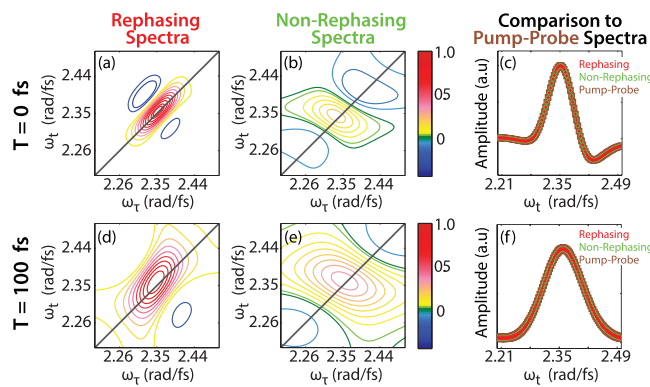


FIG. 1. Comparison of simulated 2D data to pump probe spectra. Top row: (a) rephasing, (b) non-rephasing, and (c) comparison of projections of rephasing (red “+”) and non-rephasing (green circles) signals to pump-probe signal (brown square) for $T = 0$ fs. Bottom row: (d) rephasing, (e) non-rephasing, and (f) comparison of projections of rephasing (red “+”) and non-rephasing (green circles) signals to pump-probe signal (brown squares) for $T = 100$ fs.

The purpose of phasing 2D spectra using spectrally resolved pump-probe signals is to correctly identify the absorptive and dispersive components of the susceptibility tensor in the frequency domain. Correct identification of absorptive and dispersive components can also be achieved in time domain by time-resolved heterodyne detection of transient grating (TG) signal.¹⁹ In this method, the time dependence of absorptive and dispersive components can be obtained by systematically varying the phase between the TG signal and the LO, resulting in complete characterization of absorptive and dispersive components. A variant of this approach has recently been applied to phasing of 2D electronic spectra by Hauer and co-workers.²⁰

III. EXPERIMENTAL METHOD

GRAPES has been employed to acquire rephasing signal in the $-\vec{k}_1 + \vec{k}_2 + \vec{k}_3$ direction, where \vec{k}_1 , \vec{k}_2 , and \vec{k}_3 are the wave vectors of the three excitation pulses 1–3, respectively.^{13,14} The geometry for acquiring rephasing signal has been discussed in detail previously.^{13,14} Briefly, a Coherent Micra Ti:sapphire oscillator seeds a Coherent Legend

Elite USP-HE regenerative amplifier to generate 30 fs, transform-limited pulses centered at 805 nm (30 nm FWHM) with a 5 kHz repetition rate. A 50:50 beam splitter splits the output of the regenerative amplifier. One of the beams is incident on a retroreflector mounted to a motorized translational stage to generate the waiting time (T). The other beam is incident on a stationary retroreflector, appropriately adjusted to compensate for distance. Both beams then reflect off the front and back surfaces of a coated 3 mm, 3° wedged optic ($R_1 = 40\%$, $R_2 = 60\%$). The first four reflections generate excitation pulses 1–3 and the LO 4 in the rephasing direction as shown in Figure 2(a). We additionally use another internal reflection to create beam 4' for the non-rephasing local oscillator (Figure 2(a)). Beams 2 and 3 travel through 6 mm of glass in the wedged optic, which is taken into account by compensating beam 1 with 6 mm fused silica placed in its path. The coatings ensure that the three excitation pulses have similar power. The beams are directed toward the sample by the GRAPES mirror assembly (Figures 2(c) and 2(d)) in boxcars and distorted boxcars geometries to acquire signals in the non-rephasing and rephasing directions, respectively (Figure 2(b)). The beams are focused to a 6 mm line at the sample using a 250 mm focal length cylindrical lens. The emitted signal is focused into a 15 μm slit using a pair of 25 cm and 50 cm focal length concave mirrors. The signal is spectrally resolved using a 600 lines/mm diffraction grating and imaged onto a 2048 \times 2048 thermally cooled CCD array (Andor). The rephasing and non-rephasing signals were acquired separately. Figures 3(a) and 3(b) compare the raw, heterodyned rephasing and non-rephasing signal imaged on the camera for zero waiting time. The colorbar indicates the counts generated on the CCD camera. As expected, the rephasing and non-rephasing signals are of similar intensity for zero waiting time. The fringe contrast of the signal-LO interferogram was optimized by varying the power of LO using a variable metallic neutral density filter introduced in the path of the LO. Timing between pulses was determined using spectral interferometry as described by Lepetit.²¹ The precise location of $\tau = 0$ is important for our phasing approach. A detailed description of how pulse timings are determined in GRAPES has been given by Harel.¹⁴ Figure S3

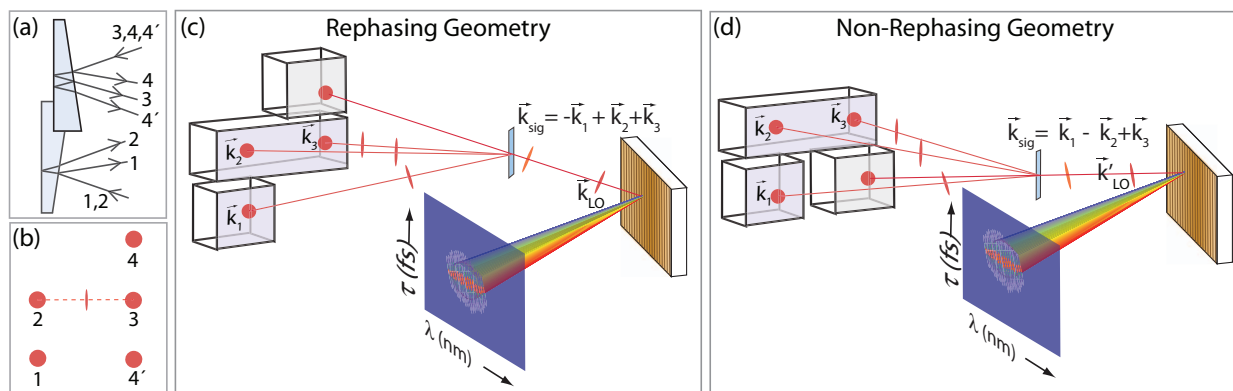


FIG. 2. Optical apparatus to acquire rephasing and non-rephasing signals from GRAPES. (a) The wedged optic arrangement to produce all the required beams 1, 2, 3, 4, and 4'. (b) Beams 1, 2, 3, and 4 form parallelogram boxcar geometry, while beams 1, 2, 3, and 4' form a boxcar geometry. The beams are focused at the center of the line joining 2 and 3. (c) GRAPES mirror assembly for acquiring rephasing signal. (d) Modified GRAPES mirror assembly for acquiring non-rephasing signal.

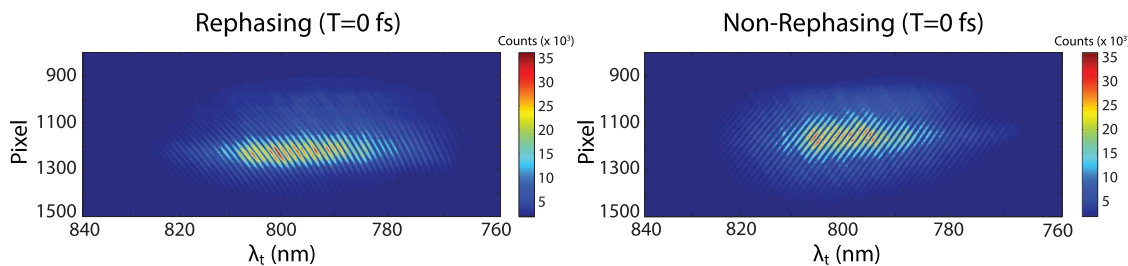


FIG. 3. Raw heterodyned rephasing (a) and non-rephasing (b) signals for zero waiting time. The colorbar indicates the counts generated on the CCD camera.

of the supplementary material¹⁵ shows a brief overview the timing calibration procedure and timing data for the present experiments.

Data processing of nonlinear, third-order 2D optical signals has been described in detail by Brixner *et al.*¹⁰ An adaptation of the analysis for rephasing signals acquired using GRAPES has been described by Harel.¹⁴ Non-rephasing spectra were processed by the same procedure.

With a pulse energy of 60 nJ/pulse, we achieve a fluence of $14 \mu\text{J}/\text{cm}^2$, which is comparable to the fluence used in conventional 2D experiments.²² Only a small fraction of the beam, less than 1 mm, is required for data acquisition (see the supplementary material¹⁵ for explanation). We assume constant power over 1 mm near the center of the Gaussian beam.

Pump-probe data, for phasing, was acquired using GRAPES apparatus as well. To acquire the pump-probe signal, beam 2 was used as pump and beam 3 was used as probe while other beams were blocked.^{13,14} For all experiments, the sample consisted of a flowing solution of 0.3 M IR144 (O.D. = 0.22) in methanol in 200 μm thick fused silica flow cell (Starna).

IV. RESULTS AND DISCUSSION

The complex 2D spectra acquired in the rephasing and non-rephasing directions was phased as shown

$$PP(T, \omega_t) = A \cdot \text{Re} \left\{ \int_{-\infty}^{+\infty} d\omega_\tau S^{(3)}(\omega_\tau, T, \omega_t) \times \exp(i\phi_c + i(\omega_t - \omega_o)t_c + i(\omega_t - \omega_o)^2 t_d^2) \right\}, \quad (4)$$

where A is a normalization constant, ϕ_c is the constant phase, and $(\omega_t - \omega_o)$ is the rephasing frequency in the rotating frame of the field which oscillates at ω_o center frequency. The term t_c corrects for uncertainty in the timing between the pulses 3 and LO, and the term t_d is a fitting parameter that corrects for the phase distortions in the LO resulting from variable metallic neutral density introduced in the path of LO to optimize fringe contrast of the signal-LO interferogram on the camera.²³ Independently phased signals in the rephasing and non-rephasing directions, $-\vec{k}_1 + \vec{k}_2 + \vec{k}_3$ and $+\vec{k}_1 - \vec{k}_2 + \vec{k}_3$, respectively, are presented in Figure 4. In order, the top row of Figure 4 shows phased rephasing, non-rephasing, and comparison of the projections of both to pump-probe signal for $T = 0$ fs. The bottom row shows these same spectra for

$T = 100$ fs. For early waiting times ($T = 0$ fs) absorption and emission frequencies are correlated, resulting in diagonally elongated peaks (Figures 4(a) and 4(b)). After the waiting time increases to $T = 100$ fs, absorption and emission frequencies lose correlation due to solvent dynamics, resulting in more rounded peaks (Figures 4(d) and 4(e)).

The diagonal, positive feature in Figure 4 results from stimulated emission and ground state bleach. In these rephasing and non-rephasing spectra, the negative, off-diagonal features result primarily from dispersive contributions and are a concomitant outcome of Fourier transforming the signal over two time domains.^{24,25} The frequency-resolved pump-probe signal is superimposed with probe-scatter interference. The interference is more prominent at shorter waiting times than longer waiting times. Due to these additional effects at early times, the signals fit better to their corresponding pump-probe spectra for $T = 100$ fs than for $T = 0$ fs, as shown in Figures 4(c) and 4(f). The projections of the signals compare better for $T = 100$ fs than for $T = 0$ fs.

The scaling factor and the phase parameters from Eq. (4), obtained after individually phasing the signals in the rephasing and non-rephasing directions to the pump-probe signal, ensure that the signals are equal for zero coherence time, hence suitably normalizing the two signals for comparison. The purely absorptive spectrum (Figures 5(a) and 5(c)) is obtained by adding the phased rephasing and non-rephasing spectra. However, because the signals in the

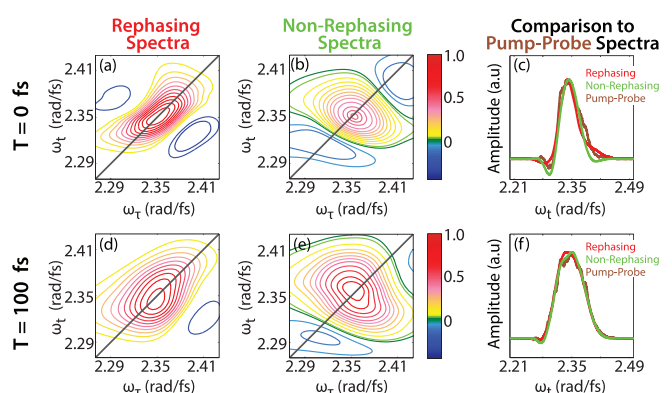


FIG. 4. Comparison of experimental 2D rephasing and non-rephasing spectra to pump probe data. Top row: (a) rephasing signal, (b) non-rephasing signal, and (c) projection of rephasing signal (red) and non-rephasing signal (green) to pump-probe signal (brown) for $T = 0$ fs. Bottom row: (d) rephasing signal, (e) non-rephasing signal, and (f) projection of rephasing signal (red) and non-rephasing signal (green) to pump-probe signal (brown) for $T = 100$ fs.

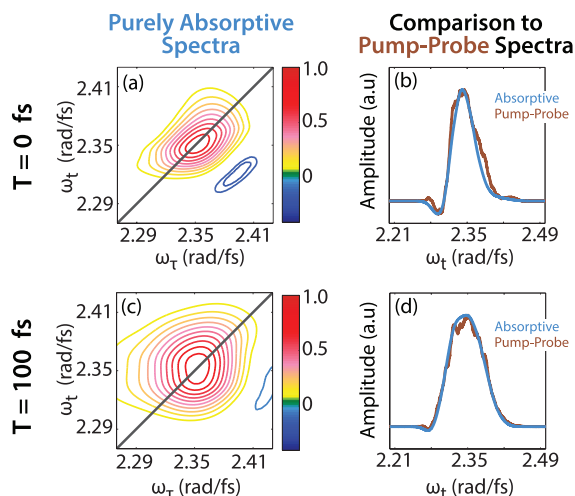


FIG. 5. Comparison of purely absorptive GRAPES spectra to pump-probe data. Top row ($T = 0 \text{ fs}$): (a) purely absorptive spectra and (b) comparison of the projection of the purely absorptive spectrum (blue) with pump-probe spectrum (brown). Bottom row ($T = 100 \text{ fs}$): (c) purely absorptive spectra and (d) comparison of the projection of the purely absorptive spectrum (blue) with pump-probe spectrum (brown).

rephasing and the non-rephasing directions were phased individually to the pump-probe signal, the projection of the purely absorptive spectrum is twice the pump-probe signal. The purely absorptive spectrum was therefore divided by 2 to obtain the absorptive 2D spectra presented in Figures 5(a) and 5(c).

The projections of the purely absorptive spectrum (blue) to the pump-probe signal (brown) are compared in Figures 5(b) and 5(d). The diagonal feature on the purely absorptive spectrum is elongated for early waiting times ($T = 0 \text{ fs}$, Figure 5(a)) stemming from correlated absorption and signal emission frequencies. For longer waiting times, solvent dynamics cause the system to lose correlation between absorption and emission frequencies. This loss of memory results in a rounder diagonal feature for $T = 100 \text{ fs}$ (Figure 5(c)). The purely absorptive feature is free from phase twist, and the residual off diagonal negative features can be attributed to vibrational wave packet motion on the ground or excited electronic state as described by Gallagher Faeder and Jonas.²⁶

V. CONCLUSION

We show that the signals in the rephasing and non-rephasing directions can be phased independently using frequency-resolved pump-probe spectra. Furthermore, GRAPES has been demonstrated to acquire signal in the non-rephasing direction. The signals in the rephasing and the non-rephasing directions, acquired using GRAPES, were phased independently resulting in the reconstruction of purely absorptive 2D spectra. Our results were found to be in good

agreement with previous studies. This advance opens the possibility of mapping real time evolution of the Hamiltonian of systems that evolve during data acquisition.

ACKNOWLEDGMENTS

The authors thank NSF MRSEC (DMR 08-02054), AFOSR (FA9550-09-1-0117), DTRA (HDTRA1-10-1-0091), and the DARPA QuBE program (N66001-10-1-4060) for partially supporting this work. A.F.F. thanks the DOE SCGF program for funding.

- ¹K. W. Stone, K. Gundogdu, D. B. Turner, X. Li, S. T. Cundiff, and K. A. Nelson, *Science* **324**(5931), 1169–1173 (2009).
- ²G. B. Griffin, S. Ithurria, D. S. Dolzhnikov, A. Linkin, D. V. Talapin, and G. S. Engel, *J. Chem. Phys.* **138**(1), 014705 (2013).
- ³A. Nemeth, F. Milota, J. Sperling, D. Abramavicius, S. Mukamel, and H. F. Kauffmann, *Chem. Phys. Lett.* **469**(1–3), 130–134 (2009).
- ⁴T. Brixner, J. Stenger, H. M. Vaswani, M. Cho, R. E. Blankenship, and G. R. Fleming, *Nature (London)* **434**(7033), 625–628 (2005).
- ⁵C. Y. Wong, R. M. Alvey, D. B. Turner, K. E. Wilk, D. A. Bryant, P. M. G. Curmi, R. J. Silbey, and G. D. Scholes, *Nat. Chem.* **4**(5), 396–404 (2012).
- ⁶G. S. Engel, T. R. Calhoun, E. L. Read, T.-K. Ahn, T. Mancal, Y.-C. Cheng, R. E. Blankenship, and G. R. Fleming, *Nature (London)* **446**(7137), 782–786 (2007).
- ⁷S. Mukamel, *Principles of Nonlinear Optical Spectroscopy* (Oxford University Press, New York, 1995).
- ⁸J. D. Hybl, A. A. Ferro, and D. M. Jonas, *J. Chem. Phys.* **115**(14), 6606–6622 (2001).
- ⁹M. L. Cowan, J. P. Ogilvie, and R. J. D. Miller, *Chem. Phys. Lett.* **386**(1–3), 184–189 (2004).
- ¹⁰T. Brixner, T. Mancal, I. V. Stiopkin, and G. R. Fleming, *J. Chem. Phys.* **121**(9), 4221–4236 (2004).
- ¹¹M. Cho, H. M. Vaswani, T. Brixner, J. Stenger, and G. R. Fleming, *J. Phys. Chem. B* **109**(21), 10542–10556 (2005).
- ¹²R. M. Hochstrasser, *Proc. Natl. Acad. Sci. U.S.A.* **104**(36), 14190–14196 (2007).
- ¹³E. Harel, A. F. Fidler, and G. S. Engel, *Proc. Natl. Acad. Sci. U.S.A.* **107**(38), 16444–16447 (2010).
- ¹⁴E. Harel, A. F. Fidler, and G. S. Engel, *J. Phys. Chem. A* **115**(16), 3787–3796 (2011).
- ¹⁵See supplementary material at <http://dx.doi.org/10.1063/1.4818808> for details on pulse ordering and the projection slice theorem.
- ¹⁶D. M. Jonas, *Annu. Rev. Phys. Chem.* **54**(1), 425–463 (2003).
- ¹⁷R. N. Bracewell, *The Fourier Transform And Its Applications* (McGraw-Hill, USA, 1999).
- ¹⁸T. Joo, Y. Jia, J.-Y. Yu, M. J. Lang, and G. R. Fleming, *J. Chem. Phys.* **104**(16), 6089–6108 (1996).
- ¹⁹G. D. Goodno, G. Dadusc, and R. J. D. Miller, *J. Opt. Soc. Am. B* **15**(6), 1791–1794 (1998).
- ²⁰F. Milota, C. N. Lincoln, and J. Hauer, *Opt. Express* **21**(13), 15904–15911 (2013).
- ²¹L. Lepetit, G. Chériaux, and M. Joffre, *J. Opt. Soc. Am. B* **12**(12), 2467–2474 (1995).
- ²²G. Panitchayangkoon, D. Hayes, K. A. Fransted, J. R. Caram, E. Harel, J. Wen, R. E. Blankenship, and G. S. Engel, *Proc. Natl. Acad. Sci. U.S.A.* **107**(29), 12766–12770 (2010).
- ²³A. W. Albrecht, J. D. Hybl, S. M. G. Faeder, and D. M. Jonas, *J. Chem. Phys.* **111**(24), 10934–10956 (1999).
- ²⁴R. R. Ernst, G. Bodenhausen, and A. Wokaun, *Principles of Nuclear Magnetic Resonance in One and Two Dimensions* (Oxford University Press, Oxford, 1987).
- ²⁵M. Khalil, N. Demirdöven, and A. Tokmakoff, *Phys. Rev. Lett.* **90**(4), 047401 (2003).
- ²⁶S. M. Gallagher Faeder, and D. M. Jonas, *J. Phys. Chem. A* **103**(49), 10489–10505 (1999).